



Strain-softening of concrete in uniaxial compression

Report of the Round Robin Test carried out by RILEM TC 148-SSC

Prepared by J.G.M. van Mier¹, S. P. Shah², M. Arnaud³, J.P. Balayssac³, A. Bascoul³, S. Choi², D. Dasenbrock⁴, G. Ferrara⁵, C. French⁴, M.E. Gobbi⁵, B.L. Karihaloo⁶, G. König⁷, M.D. Kotsovos⁸, J. Labuz⁴, D. Lange-Kornbak⁶, G. Markeset⁹, M.N. Pavlovic¹⁰, G. Simsch⁷, K-C. Thienel², A. Turatsinze³, M. Ulmer⁷, H.J.G.M. van Geel¹¹, M.R.A. van Vliet¹, D. Zissopoulos¹⁰.

(1) Delft University of Technology, Delft, The Netherlands; (2) ACBM Center, Northwestern University, IL, USA; (3) LMDC, INSA-UPS, Toulouse, France; (4) University of Minnesota, Minneapolis, MN, USA; (5) ENEL-CRIS, Milano, Italy; (6) University of Sydney, Australia; (7) Technische Hochschule, Darmstadt, Germany; (8) National Technical University of Athens, Greece; (9) SINTEF/Norwegian Defense Construction Service, Oslo, Norway; (10) Imperial College of Science, Technology and Medicine, London, UK; (11) Eindhoven University of Technology, Eindhoven, The Netherlands.

TC Membership: **Chairman:** S.P. Shah, USA; **Secretary:** J.G.M. van Mier, The Netherlands; **Members:** Z.P. Bažant, USA; N. Banthia, Canada; A. Bascoul, France; Y. Berthaud, France; A. Bittnar, Czech Republic; O. Buyukozturk, USA; A. Carpinteri, Italy; M. Elices, Spain; G. Ferrara, Italy; R. Gettu, Spain; K. Gylltoft, Sweden; M. Hassanzadeh, Sweden; N. Hawkins, USA; H. Horii, Japan; B.L. Karihaloo, Denmark; G. König, Germany; M. Kotsovos, Greece; J. Labuz, USA; G. Markeset, Norway; H.W. Reinhardt, Germany; H. Schorn, Germany; H. Stang, Denmark; K-C. Thienel, Germany; J-P. Ulfkjær, Denmark.

FOREWORD

An extensive Round Robin test programme on compressive softening was carried out by the RILEM Technical Committee 148-SSC "Test methods for the Strain Softening response of Concrete". The goal was to develop a reliable standard test method for measuring strain softening of concrete under uniaxial compression. The main variables in the test programme were the specimen slenderness h/d and the boundary restraint caused by the loading platen used in the experiments. Both high friction and low friction loading systems were applied. Besides these main variables, which are both related to the experimental environment under which softening is measured, two different concretes were tested: a normal strength concrete of approximately 45 MPa and a higher strength concrete of approximately 75 MPa. In addition to the prescribed test variables, due to individual initiatives, the Round Robin also provided information on the effect of specimen shape and size. The experiments revealed that under low boundary friction a constant compressive strength is measured irrespective of the specimen slenderness. For high friction loading systems (plain steel loading platen), an increase of specimen strength is found with decreasing slenderness. However, for slenderness greater than 2 (and up to 4), a constant strength was measured. The shape of the stress-strain curves was very consistent, in spite of the fact that each labora-

tory cast its own specimens following a prescribed recipe. The pre-peak behaviour was found to be independent of specimen slenderness when low friction loading platens were used. However, for all loading systems a strong increase of (post-peak) ductility was found with decreasing specimen slenderness. Analysis of the results, and comparison with data from literature, showed that irrespective of the loading system used, a perfect localization of deformations occurred in the post-peak regime, which was first recognised by Van Mier in a series of uniaxial compression tests on concrete between brushes in 1984.

Based on the results of the Round Robin, a draft recommendation will be made for a test procedure to measure strain softening of concrete under uniaxial compression. Although the post-peak stress-strain behaviour seems to be a mixture of material and structural behaviour, it appears that a test on either prismatic or cylindrical specimens of slenderness $h/d = 2$, loaded between low friction boundaries (for example by inserting sheets of teflon between the steel loading platen and the specimen), yields reproducible results with relatively low scatter. For normal strength concrete, the closed-loop test can be controlled by using the axial platen-to-platen deformation as a feed-back signal, whereas for high-strength concrete either a combination of axial and lateral deformation should be used, or a combination of axial deformation and axial load.

1. INTRODUCTION

In 1992, the RILEM Committee 148-SSC was founded and decided to start working on strain softening of concrete under uniaxial compression. In previous years, much work had been carried out on uniaxial tension, for example in RILEM Committees 89-FMT and 90-FMA. It was felt that uniaxial compressive softening was grossly neglected, whereas recent research carried out by Kotsovos (1983), Van Mier (1984) and Vonk (1992) showed that compressive softening might be analyzed along similar lines as tensile softening. In rock mechanics, similar results were obtained earlier, *e.g.* Hudson *et al.* (1972). As a first part of the committee's task, it was decided to organise a Round Robin test in order to confirm claims regarding size and boundary condition effects in compressive softening, and to assess variability of test results between different laboratories. The main goal of the Round Robin experiment is to develop a reliable standard test method for measuring the stress-strain diagram of concrete in uniaxial compression, including the softening diagram. In a second stage of the committee's work, analyses of strain softening in compression will be carried out.

In this report, an overview will be given of the test results obtained in 10 different test series that were carried out in laboratories in Europe, Australia and the USA. Depending on the available resources, more or less extensive test programmes were carried out by the various contributing laboratories. They are (in alphabetical order):

ACBM	NSF Center for Advanced Cement-based Materials, Northwestern University, Evanston, IL, USA.
DUT	Delft University of Technology, Stevin Laboratory, Delft, The Netherlands.
ENEL	Centro di Ricerca Idraulica e Strutturale (ENEL-Cris) Laboratories, Milano, Italy.
EUT	Eindhoven University of Technology, Eindhoven, The Netherlands.
INSA	Laboratoire Matériaux et Durabilité des Constructions, INSA-UPS, Toulouse, France.
NTUA/IC	National Technical University of Athens, Greece, in collaboration with Imperial College of Science, Technology and Medicine, London, UK.
SINTEF	SINTEF Structures and Concrete, Trondheim, Norway.
THD	Technische Hochschule Darmstadt, Institut für Massivbau, Darmstadt, Germany.
UM	University of Minnesota, Minneapolis, MN, USA.
US	University of Sydney, Sydney, NSW, Australia.

The name of each contributing laboratory has been shortened to a letter combination that will be used in the remainder of this overview.

2. TEST PROGRAMME

In 1993, the test programme (Van Mier, 1993) was accepted by the Committee. As the contributions were all financed by the individual contributing laboratories, a

minimum programme was set up. According to the available resources, the programme could be extended by each contributing laboratory. The main parameters affecting the compressive softening of concrete are:

- (1) frictional restraint between the loading platen and the specimen,
- (2) the allowable rotations of the loading platens before and during the experiment,
- (3) the gauge length of the control LVDT (in a conventional displacement controlled test),
- (4) the stiffness of the testing machine,
- (5) the type of feed-back signal,
- (6) the loading rate,
- (7) the shape and size of the test specimen (slenderness ratio), and
- (8) the concrete composition.

Obviously, the experimental result depends on a combination of test parameters and material parameters. In particular, for softening the test parameters are difficult to separate from the material parameters. Consequently, a unique measurement of softening parameters is not a straightforward task. Because all contributors had to work with the test machines available in their laboratories, it did not make sense to base the Round Robin on a variation of machine dependent parameters (*e.g.* numbers (2) and (4)). Instead it was decided to concentrate on those parameters that are well known to have a large effect on strain-softening in compression, namely the frictional restraint between the loading platen and the specimen, and the size and shape of the test specimen. Moreover, because most compressive softening experiments carried out to date were based on normal strength gravel concrete, it was decided to perform experiments on both normal strength and high strength concrete. This is of particular interest in view of the trend to use stronger concretes in construction practice. For all other parameters, default values were suggested. Consequently, the minimum test programme was as follows:

(1) Tests had to be carried out between at least two different types of loading platens. Default was an experiment between rigid steel loading platens. The other systems to be used could be freely selected by the participant. The second system should preferably reduce the friction between loading platen and specimen to a minimum.

(2) The loading platens should be fixed against rotation during the experiment. However, before the test was to be carried out, movement of one of the platens is undoubtedly needed, as the accuracy of manufacturing the specimen is not sufficient. Some settlement is needed to ensure full contact between loading platen and specimen. A capping between the loading platen and the specimen could be used as an alternative, if adjustment of the loading platen cannot be done. It should be noted, however, that the application of a capping in combination with some friction-reducing interlayers might yield additional problems in test performance.

(3) The gauge length of the control LVDT was set equal to the specimen length. Thus, in a conventional displacement-controlled experiment, the measurements should be taken from loading platen to loading platen.

(4) As far as the stiffness of the testing machine is concerned, no default was given, because every participant was of course tied to the equipment available in his or her laboratory. At least the machine stiffness should be determined in order to facilitate comparison of the different contributions.

(5) The type of feed-back signal was the axial deformation (also see (3)). It was left to the judgement of the participant whether alternative control signals should be adopted, such as a combination of axial load and axial displacement, or a combination of lateral displacement and axial displacement. These last alternatives might be needed to successfully measure the softening branch for high strength concrete.

(6) The loading rate in all experiments should be held constant at 1 $\mu\text{m/s}$. This corresponds to a static compression test. Again, participants were free to make variations, but of course the default value should be tested.

(7) Variation of specimen size (slenderness) was considered one of the most important parameters to be studied, in combination with frictional restraint caused by the loading platens (cf. (1)). Each participant was free to choose either prismatic specimens or cylindrical specimens with a constant cross-sectional area. The area for the prisms should be 100 x 100 mm^2 , whereas the diameter of the cylinder cross-section should be equal to 100 mm. Different slenderness ratios were then obtained by varying the length of the specimens from 50, 100 to 200 mm. Thus, slenderness ratios $h/d = 0.5, 1.0$ and 2.0 were to be tested. The participants were free to add experiments on specimens of different cross-sectional area or different shape, but the above programme was the minimum. The reason for adding the slenderness ratio $h/d = 0.5$ was that such tests would clearly show the effectiveness of the selected friction-reducing loading system.

(8) Two different concrete qualities were specified, namely a normal gravel concrete with a maximum aggregate size of 8 mm and a cube compressive strength (150 mm cubes) of approximately 40-45 MPa, and a high strength concrete with a strength of approximately 75-80 MPa.

In summary, the minimum test programme consisted of a series of uniaxial compression tests on either prisms or cylinders, loaded between two different types of loading platens. Three different slenderness ratios were to be tested using specimens of two different concrete qualities. With a repetition factor of three for each parameter combination, the minimum test programme would amount to 36 tests.

3. MATERIALS AND SPECIMEN PREPARATION

As mentioned, tests should be carried out on two different concretes. It was decided to leave the manufacturing of the specimens to the competence of the participating laboratories. A detailed manufacturing procedure was specified

[25]. Larger blocks should be cast, from which the prisms could be sawn or specimens could be cored such that the direction of loading in the compression experiments would be perpendicular to the direction of casting. As shown before by Van Mier (1984), the direction of casting has a profound effect on the shape of the stress-strain diagram in compression. Microcracks caused by differential shrinkage, temperature gradients and bleeding during the hardening of the concrete are the main reason for the initial anisotropy which cannot be neglected. In order to limit the number of experiments, a constant loading direction to casting direction was prescribed in the Round Robin proposal. Most laboratories followed this manufacturing procedure. For example, at ENEL larger blocks of 150 x 150 x 600 mm^3 were cast, from which prisms with $d = 100$ mm were sawn or cylinders with $d = 100$ mm were cored. A further advantage of testing specimens that are sawn from large blocks is that the weak top layer is removed from the specimen. The weak casting layer can, in the worst case, lead to significant flexural stresses in the test specimen. For the tests carried out at SINTEF, the cylinders were directly cast in a vertical position in plastic moulds; before testing the cylinder ends were sawn parallel. A similar procedure was followed at ACBM, INSA and at NTUA/IC. At US, prisms were cast in a vertical position in steel moulds of 425 x 100 x 100 mm^3 .

The concrete mixes to be used were specified in the Round Robin proposal as well. For the *normal strength concrete*, the composition should be as close as possible to the following recommendation: Portland cement type B (Dutch codes, resembling ASTM type III) 375 kg/m^3 ; maximum aggregate size 8 mm (preferably rounded river gravel); size distribution: 8-4 mm, 540 kg/m^3 ; 4-2 mm, 363 kg/m^3 ; 2-1 mm, 272 kg/m^3 ; 1-0.5 mm, 272 kg/m^3 ; 0.5-0.25 mm, 234 kg/m^3 ; 0.25-0.125 mm, 127 kg/m^3 ; no admixtures; w/c-ratio = 0.5. This would lead to a compressive strength of 45-50 MPa.

For the *high strength concrete*, approximately the same aggregate distribution should be aimed at, except of course that it should be corrected slightly because the amount of cement was increased to 500 kg/m^3 . Moreover, it was suggested to reduce the w/c-ratio to 0.35, to add 35 kg/m^3 of microsilica, as well as superplasticizer to obtain good workability. This would lead to a compressive strength of approximately 75-80 MPa.

The casting procedure was prescribed as well. The concrete should be poured in moulds and compacted. The specimens should be kept in the moulds for two days (48 hours). The top surfaces should be kept under wet cloths or covered by plastic to prevent drying. After demoulding the specimens should be placed in a fresh water basin. Sawing and grinding of the specimens to the prescribed size should not be done at an age earlier than 14 days. After sawing, the specimens should be returned to the fresh water basin, and at 28 days they should be removed and sealed in plastic bags. The age at loading should be between 8 and 10 weeks after casting.

It was not considered realistic to give more details, as local differences in the basic materials would already lead to variations in compressive strength and deformational behaviour of the concretes manufactured at the various

Laboratory	Type of test*	f_c [MPa]***	
		NSC	HSC
ACBM	cylinder 100 x 200 mm**	62.7	83.6
DUT	cube 150 mm	53.8	84.9
ENEL	cube 150 mm	53.5	-
EUT	cube 150 mm	56.6	80.8
INSA	cylinder 118 x 220 mm/teflon	45.0	-
NTUA/IC	cube 100 mm	47.4	70.0
SINTEF	cube 100 mm	-	109.3
THD	cube 150 mm	65.0	95.0
UM	cylinder 100 x 200 mm	52.0	75.0
US	cylinder 150 x 300 mm	43.0	-

*) end condition plain steel platen except when stated otherwise.

**) age 56 days.

***) strength for NSC and HSC respectively.

participating laboratories. In all reports submitted by the participants, the concrete compositions used were specified in more or less detail. Because there was no uniform format, we limit the presentation here to Table 1, in which the 28 day compressive strengths obtained are summarized.

It should be mentioned that not all participants carried out experiments on two different concretes as was requested. Table 1 clearly shows what was done. The tests at SINTEF were not according to the Round Robin proposal, but they give some insight into the behaviour of concrete with a uniaxial compressive strength over 100 MPa. For the rest, the average uniaxial compressive strength for the NSC lay between 43.0 and 65.0 MPa, for the HSC between 70.0 and 109.3 MPa. As a result, a rather continuous range of concretes was obtained. In spite of the prescribed compositions, large differences in strength are still found. The differences in deformational behaviour are sometimes even larger, but these will be discussed further on in the paper.

4. SPECIMENS AND LOADING EQUIPMENT

4.1 Specimens

As mentioned, the participants were free to select prismatic or cylindrical specimens. Model codes require testing of cylindrical specimens in some countries, whereas cubes or other prismatic shapes are used elsewhere. In order to be consistent with current practice, the shape was not prescribed. Prisms were tested at DUT, ENEL, EUT, THD, NTUA/IC and US; cylinders were used at ACBM, ENEL, INSA, THD, SINTEF and UM. The above indicates that both prisms and cylinders were tested at ENEL and THD, giving the opportunity to verify whether the shape of the specimen has any significant influence on strength and stress-strain behaviour. In spite of the request for 100 mm diameter

Slenderness h/d	Participants
$h/d = 0.5, 1, 2$ $h/d = 0.25, 0.5, 1, 2$ $h/d = 1, 2, 3$ $h/d = 2, 3, 4$ $h/d = 1, 2$ $h/d = 2$	ENEL, EUT, THD, UM DUT ACBM SINTEF INSA, US NTUA/IC
Specimen diameter d^*	Participants
$d = 50$ mm $d = 75$ mm $d = 100$ mm	ENEL NTUA/IC ACBM, DUT, ENEL, EUT, SINTEF, THD, UM, US
$d = 118$ mm $d = 150$ mm	INSA ENEL

*) d is either the diameter of a cylinder or the width of a prism, depending on which geometry is used.

cross-section of prisms and cylinders, the size deviated from this requirement in several cases. In Table 2 an overview is given of the slenderness ratios and absolute diameters of the specimens in the various laboratories.

In summary, the slenderness range was extended from $h/d = 0.25$ (DUT) to $h/d = 4.0$ (SINTEF), whereas the size ranged from $d = 50$ mm to $d = 150$ mm. In comparing the different test series, care must be taken that specimens of the same size are compared to one another.

4.2 Loading platens

As mentioned before, each participant was asked to perform tests both between rigid steel platens and between a loading platen system with friction-reducing ability. The rigid loading platen was to have the same size as the concrete specimen, *i.e.* the same diameter for cylinders and the same square cross-section for cubes and prisms. The frictionless loading system was to be selected by each individual participant. As a result, quite a number of different friction-reducing systems were used; they are summarised in Table 3. The application of teflon interlayers between the steel platen and the concrete specimen was quite popular. However, the various teflon interlayers varied widely, as can be seen in Table 3.

In most cases, the loading platen had exactly the same size and shape as the specimens' cross-section. As can be seen, the friction-reducing measures varied considerably between the different test series, but this has added to a better understanding of fracturing of concrete in compression. Of particular interest are the experiments where different types of teflon interlayers were used. Inserting one or two sheets of teflon between the steel loading platen and the concrete specimen is a simple and effective method to reduce end friction, as will be shown in Section 5.2. It should be mentioned that applying grease between the loading platen and specimen may cause erroneous results. If too much grease is applied, the excess material will squeeze out in the beginning of the test, thereby exerting a tensile splitting force at the top and bottom parts of the

Table 3 – Friction-reducing loading systems used by the various participants in the Compressive Round Robin		
Participant	Rigid loading platen	Lubricated loading platen
ACBM	steel	- steel with stearic acid
		- steel with one 50 mm teflon sheet plus bearing grease
DUT	steel	- steel plus two sheets of 100 mm teflon sheets plus 50 mm grease in between
ENEL	steel	- steel plus one 500 mm teflon sheet
EUT	steel	- steel plus one 50 mm teflon sheet, with grease between teflon and steel platen
INSA	steel	- steel plus 2 sheets of 1000 mm teflon
		- steel plus aluminium strips and talc powder
		- steel plus brass strips and talc powder
NTUA/IC	steel	- steel plus a layer of 0.75 mm synthetic rubber
		- steel plus MGA pads (sandwich of 0.2 mm hardened aluminium, moly slip grease and Melinex polyester film (gauge 100))
		- brush platens (bristle length 75 mm)
SINTEF	steel	-
THD	steel	- steel plus two 50 mm teflon sheets with teflon oil in between
UM	steel	- steel plus stearic acid lubricant
US	steel	- steel plus one 127 mm teflon sheet
		- steel plus one 250 mm teflon sheet

specimen, as shown schematically in Fig. 1. As a result, the apparent strength may decrease, and the “true compressive strength” is not measured (whatever that may be). Note, however, that the effect may be somewhat diminished when grease is squeezed in the surface pores. Again, this ‘advantage’ must be judged with some care because premature splitting of the concrete specimens might occur when grease is squeezed in surface pores. When plain steel platens are used, triaxially-confined zones develop in the parts of the specimen in contact with the loading platens (see left part of Fig. 1).

4.3 Test machine

In the Round Robin proposal, it was prescribed that all tests should be carried out between fixed loading platens, *i.e.* non-rotatable platens. It was suggested that a hinge could be used at one end, but only to adjust the loading system to the specimen in case of deviating specimen shape and size. The various reports reveal that in almost all laboratories a testing machine was available with a spherical seat or hinge at one end of the specimen. The report from UM states that tests were carried out between fixed platens. At THD, a hinge was available above the upper loading platen, but in spite of this, quite some scatter in results was obtained. Next to the THD results, the strength data from UM also showed large scatter, which might be explained by geometrical imperfections (problems in plane-parallelity which were reported by the THD group) of the specimens and the inability of the machine to adjust to such imperfect

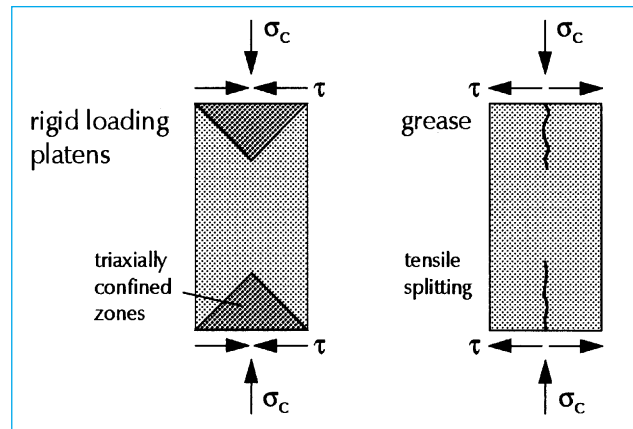


Fig. 1 – Reversal of boundary restraint when excessive grease is applied.

specimens (problematic in particular if the geometric imperfections become too large, or when a machine with two fixed loading platens is used, as in the UM tests). For example, UM reports a range of Young’s moduli between 4.4 GPa and 161.3 GPa in lubricated and steel loading platen compression tests. This may indicate problems with the lubricated platens, specimen manufacturing and/or systematic problems in the test machine. Because of the large variability of the UM results, they have not been included in the comparison, although their findings on the difference between axial and circumferential test control (see Section 4.4) are in agreement with the results shown in Section 6.

In the Round Robin proposal, the participants were asked to measure the axial stiffness of their testing machine. Only limited response was received, and a comparison on the basis of this information is impossible. The effect of machine stiffness on softening is barely understood to date and should be the subject of future study.

4.4 Test control

The default control for the experiments performed was to use axial deformation as a feed-back signal in the closed-loop servo-controlled loading system. For high strength concrete, it is known that the large energy release during failure may produce snap-back behaviour, leading to unstable regimes in the softening branch, see for example Rokugo *et al.* (1986) and Glavind and Stang (1991). The problem of snap-back is further increased when anti-frictional materials are used and as specimens become longer and more slender. The use of axial deformation as the feed-back signal is not always appropriate for controlling the test during the post-peak regime when snap-back occurs, or even when the post-peak curve is very steep. Another feed-back signal which continuously increases in time should be used. Examples are a combination of axial deformation and axial load, as was proposed by Okubo and Nishimatsu (1985), or one might use the lateral (or circumferential) deformation instead. Shah *et al.* (1980) were the first to use circumferential expansion as a feed-back signal for high strength concrete subjected to uniaxial

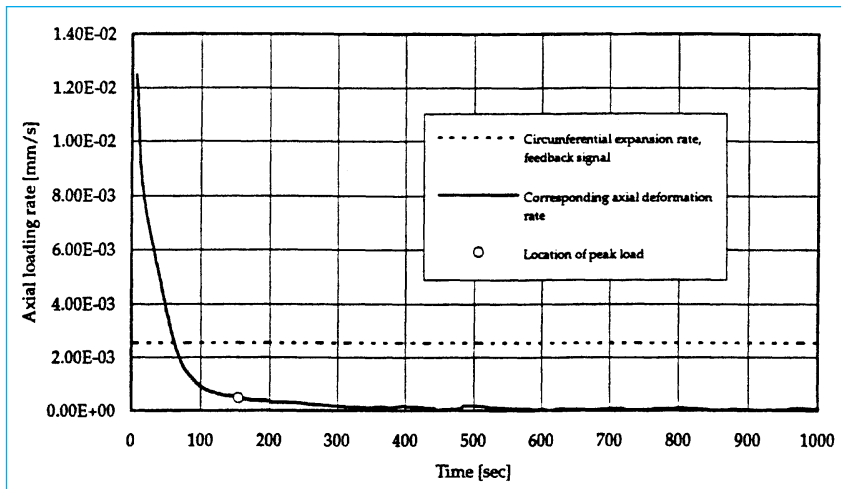


Fig. 2 – Circumferential and axial loading rates from compression tests carried out at ACBM, after Choi *et al.* (1994).

compression. The system was later used by others too, for example Taerwe (1992) and Jansen *et al.* (1995). In the Round Robin test-programme, both ACBM and UM performed tests using circumferential deformation control. The relation between axial loading rate and time under circumferential strain control is shown in Fig. 2. The circumferential strain is defined as the circumferential displacement divided by the undeformed circumference. With a constant circumferential expansion rate, the axial loading rate varies from a very fast loading in the beginning of the experiment, to a substantially lower loading rate beyond peak (in Fig. 2, the peak is indicated by an open circle). The problem of widely varying axial loading rate when circumferential (or lateral) control is used is discussed in further detail by Jansen *et al.* (1995).

To overcome the problem of widely-varying axial loading rate, Glavind and Stang (1991) proposed to use a proportional combination of axial deformation and circumferential expansion as the feed-back signal. This combination was also used by Dahl and Brincker (1989), Choi (1996) and by THD and SINTEF in the present Round Robin programme. In the pre-peak regime, when the lateral or circumferential expansion is small, the axial deformation dominates the feed-back signal. However, in the post-peak regime, the circumferential strain is sufficiently large to stabilise the feed-back signal when snap-back occurs in the stress-axial displacement curve. The proper ratio with which to combine the axial and lateral displacements must be determined based on specimen size, end conditions and type of concrete.

Instead of the circumferential expansion which is used for cylindrical specimens only, discrete lateral displacements in tests on prismatic specimens can be used as well (*e.g.* Han and Walraven (1993) and Choi (1996)). The main problem with these methods using circumferential expansion or lateral displacements in the feed-back signal is capturing the location where the lateral expansion occurs. For specimens with $h/d < 2$, this is generally no problem, especially when rigid loading platens are used. However, for more slender specimens and also when lubricated loading platens are used, locating the critical failure region may

be problematic. A proper averaging procedure is needed, because a specimen will disintegrate into a larger or smaller number of discrete parts which may give rise to widely-varying lateral deformations, see Van Mier (1984).

An alternative feed-back signal is a combination of axial displacement and axial load, originally introduced by Okubo and Nishimatsu (1985) for testing rocks in compression. The same system was used by others for concrete compression tests, *e.g.* Rokugo *et al.* (1986), Jansen and Shah (1997), and by EUT in this Round Robin programme. The so-called Partial-Elastic-Subtraction-Method (PESM) uses the axial displacement of the specimen and

subtracts an amount of the force which corresponds to a fraction of the elastic response of the specimen to give a stable feed-back signal as shown in Fig. 3. The feed-back signal S is:

$$S = \delta - \alpha F/K_0$$

where δ is the displacement in [mm], F is the force in [kN], K_0 is the initial stiffness in [kN/mm], and α is the fraction of the elastic specimen response to be subtracted ($0 \leq \alpha \leq 1$). Note that when $\alpha = 0$, S is the same as using the displacement δ as the feed-back signal. When $\alpha = 1$, the feed-back signal does not change during the initial portion of the loading ramp (when $\Delta F/\Delta \delta = K_0$). Severe snap-back occurred in the test shown in Fig. 3: the displacement decreased significantly after the peak load. An

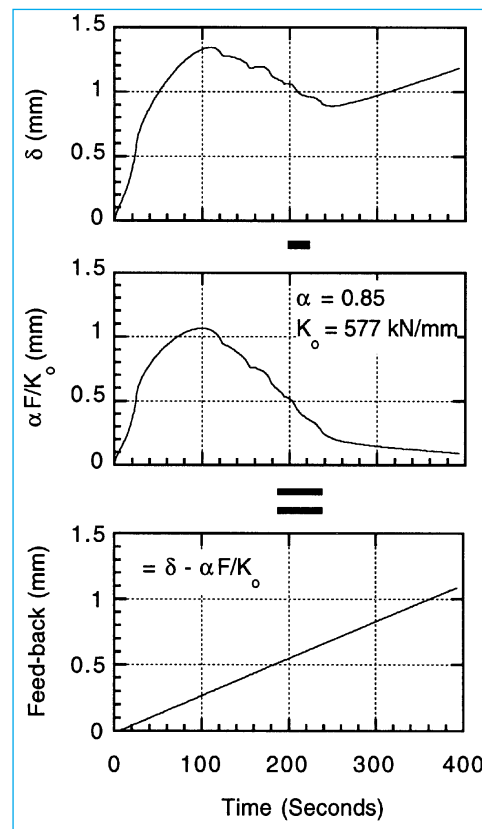


Fig. 3 – Composition and addition of the PESM feed-back signal, after Jansen and Shah (1997).

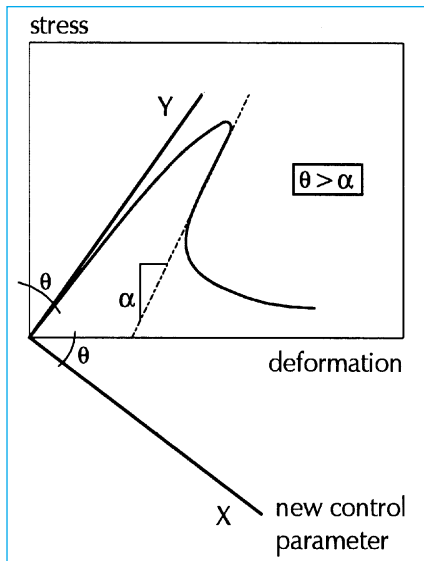


Fig. 4 – Rotation of axis for combined force/displacement control, after Van Mier (1997).

alternative view of this method is to consider the ‘feed-back axis’ as an axis rotated from the displacement axis such that the curve described by the force and displacement always increases relative to this ‘feed-back axis’ as shown in Fig. 4. See Jansen and Shah (1997) for more information about these methods.

5. EXPERIMENTAL RESULTS

The results of the various experiments were all reported in detail. References to these reports are included at the end of the paper. The most extensive test-series were carried out at ACBM, DUT, ENEL, EUT and THD. The scope of the other test series was more limited, but provided substantial information as well. In this section, the results will be described and compared. It is unavoidable that all the information must be condensed, and it is not possible to include every detail of all test-series in this paper. The interested reader is referred to the original reports prepared by the various participants. Below, the information is limited to the strength results (Section 5.1), the effects of slenderness and boundary restraint on the stress-strain behaviour in compression (Section 5.2), the effect of the specimen shape and size (Section 5.3), and the localization of deformations in the softening regime (Section 5.4).

5.1 Effect of slenderness and boundary restraint on strength

In Figs. 5 and 6, an overview is given of the strength results from the five largest test series (ACBM, DUT, ENEL, EUT and THD). In Fig. 5 a comparison is made for tests carried out between rigid steel platens, whereas

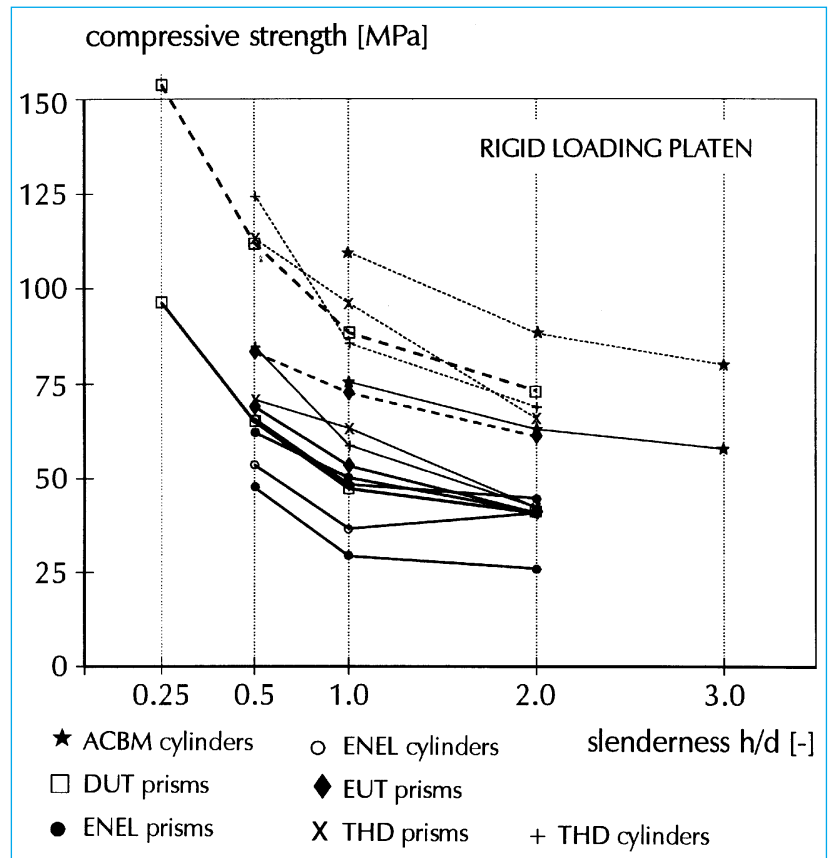


Fig. 5 – Effect of specimen slenderness on the uniaxial compressive strength when rigid steel platens are used.

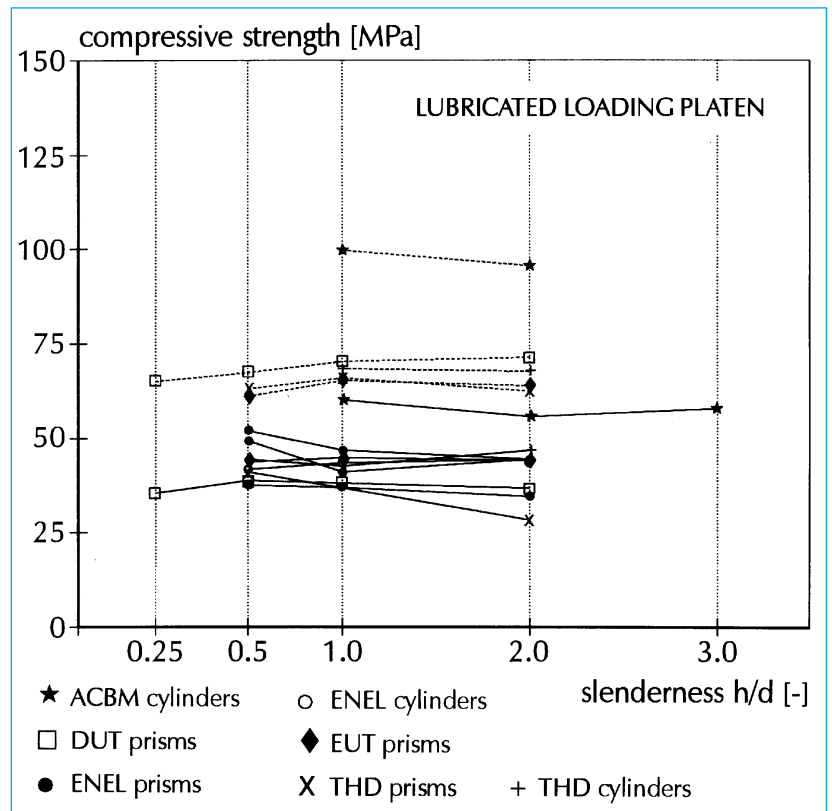


Fig. 6 – Effect of specimen slenderness on the uniaxial compressive strength when lubricated platens are used.

in Fig. 6, a comparison is made for tests between lubricated loading platens. Basically the results confirm tendencies reported earlier in the literature (see, for example, Schickert (1980)).

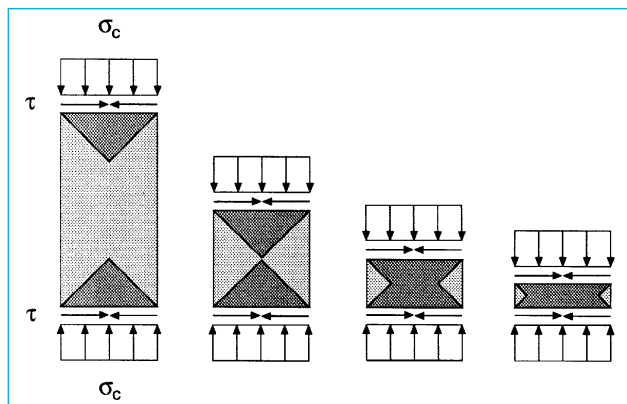


Fig. 7 – Confined zones due to frictional restraint for specimens of different slenderness, after Van Vliet and Van Mier (1996).

When rigid steel platens are used, the apparent compressive strength of the concrete, or rather the specimen strength, increases when the slenderness decreases. The strength decrease stops when the slenderness is larger than 2–2.5. Schickert showed earlier that for further increasing slenderness ratios a very slight increase of specimen strength occurs. For very large ratios, it is expected that other mechanisms like buckling will become more prominent. When lubricated loading platens are used, the increase of specimen strength does not occur, but rather constant strength is measured. Most test-series showed this tendency, as can be seen from Fig. 6. A (more or less) constant relationship was found between strength and slenderness. The explanation of the increase of strength must be sought in the frictional restraint that will build up during a test when rigid loading platens are used. The shear stresses between loading platen and specimen are caused from a mismatch in lateral expansion and stiffness of the loading platen and specimen, as explained by many authors, *e.g.* Gerstle *et al.* (1978), Schickert (1980), Kotsovos (1983) and Van Mier (1984). As a consequence, triaxially-confined regions develop in the specimens as shown schematically in Fig. 7. The restrained zones include most of the specimen at small slenderness, whereas relatively large unrestrained areas develop when the specimen height increases. Thus, a higher strength must be measured at low h/d , because the triaxial compressive strength is normally assumed to be larger than the uniaxial compressive strength. It should be noted that in triaxial experiments, constraint effects may play a larger or smaller role as well.

Crack growth usually is limited to the unconfined regions. This was demonstrated by all participants. The well-known hour-glass failure mode was observed in the constrained tests, whereas crack growth was distributed over the entire specimen's volume in the tests where friction reducing measures were employed, see for example Van Vliet and Van Mier (1996).

5.2 Effect of slenderness and boundary restraint on stress-strain behaviour

The various test series gave detailed information on the stress-strain behaviour in compression. Both axial and lateral strains were recorded by most participants. Results

were presented in different ways, namely as individual stress-strain curves, as normalised stress-strain curves, or as average stress-strain diagrams of three tests. Because the concretes used by the different participants led to different strength (Figs. 5 and 6) and deformational behaviour, it was decided not to present all stress-strain data in a single diagram, but rather to investigate whether similar phenomena were found. In general, the conclusion seems that the various mechanisms presented below were confirmed in the 10 different test series. First, the slenderness effect is discussed by means of the experimental results from EUT, DUT, THD and SINTEF. Next, the influence of boundary restraint is presented using data from INSA, NTUA/IC and US. A comparison of cylinder tests and prism tests based on data from ENEL and THD is included in Section 5.3.1. The effect of specimen size on stress-strain behaviour is discussed in Section 5.3.2.

The stress-strain curves that are included here were taken directly from the submitted reports and no further corrections were made. In some cases, like that of ENEL, the curves are averages from three experiments. In other cases, like DUT and EUT, single response curves are shown. In these cases, the middle curve of three stress-strain diagrams is shown.

5.2.1 Effect of specimen slenderness

The influence of specimen slenderness on the compressive stress-strain behaviour of normal and high strength concrete has been summarised in three sets of diagrams, *i.e.* Figs. 8, 9 and 10. Each figure consists of four diagrams, namely the upper two for normal strength concrete and the lower two for high strength concrete. For each material, tests between steel platens (high friction) are included in the two diagrams at the left (a,c). The tests between lubricated platens (low friction) are presented in the two graphs at the right (b,d). The strain is shown up to 20‰ except for the experiments carried out at DUT, where the scale was elongated to 40‰.

In Fig. 8 the results of cylinder tests carried out at THD under normal axial strain control are shown. In Fig. 9 the results from EUT are summarised, and Fig. 10 presents the stress-strain data from DUT. In Fig. 8, each curve is the average of three tests, whereas in Figs. 9 and 10 single response curves (*i.e.* the middle curve of a set of three) are shown.

The results all show the same tendency. With decreasing slenderness, the strength increases when steel platens are used, and the stress-strain curve indicates a more ductile behaviour. This can be seen clearly from Figs. 8a,c, 9a,c and 10a,c. The increase of strength for tests carried out between rigid steel platens was shown before in Fig. 5. If teflon or other lubricating loading platens are used, the increase of strength is found to disappear, but the differences in post-peak ductility with variation of the specimen slenderness remain (although slightly less pronounced). The results of EUT and DUT show this tendency most clearly. Others, like ACBM, SINTEF, ENEL and UM, found the same increase of ductility with decreasing specimen slenderness.

The THD results showed unstable softening response for the 200 mm-high specimens of high strength concrete

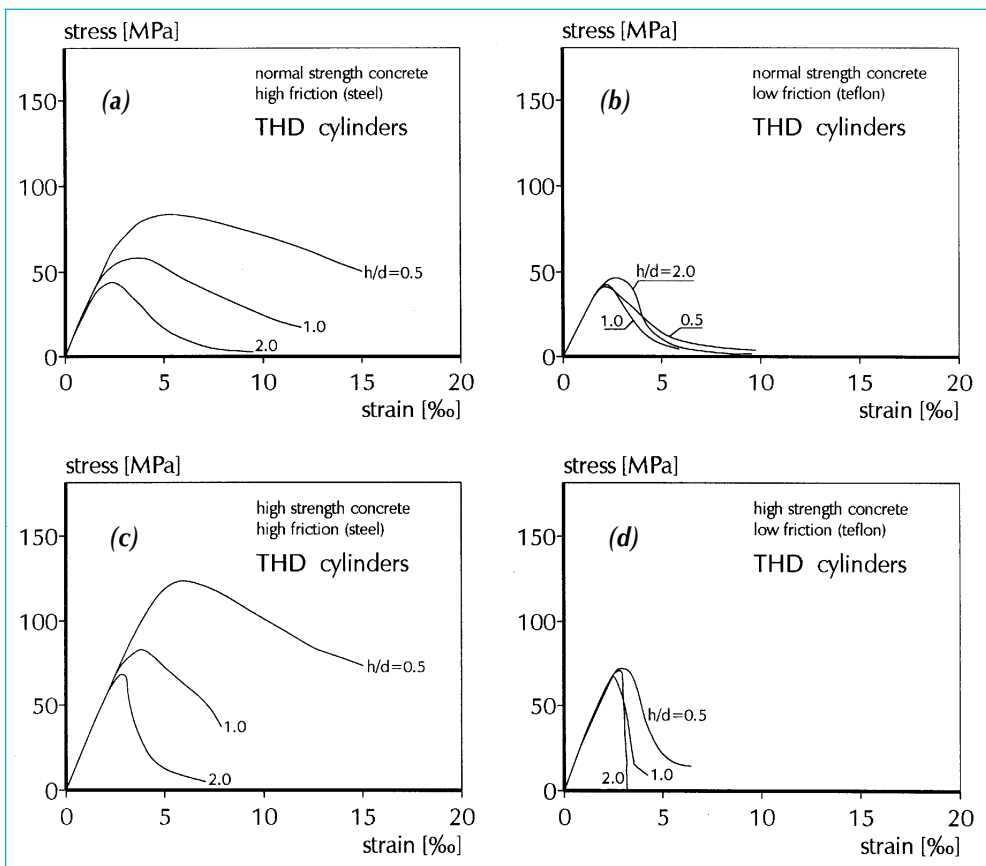


Fig. 8 – Stress-strain curves from cylinder tests at THD. Fig. (a) shows the results for normal strength concrete loaded between steel platens, (b) normal strength concrete between teflon platens, (c) high strength concrete between steel platens, and (d) high strength concrete between teflon platens, after König *et al.* (1994).

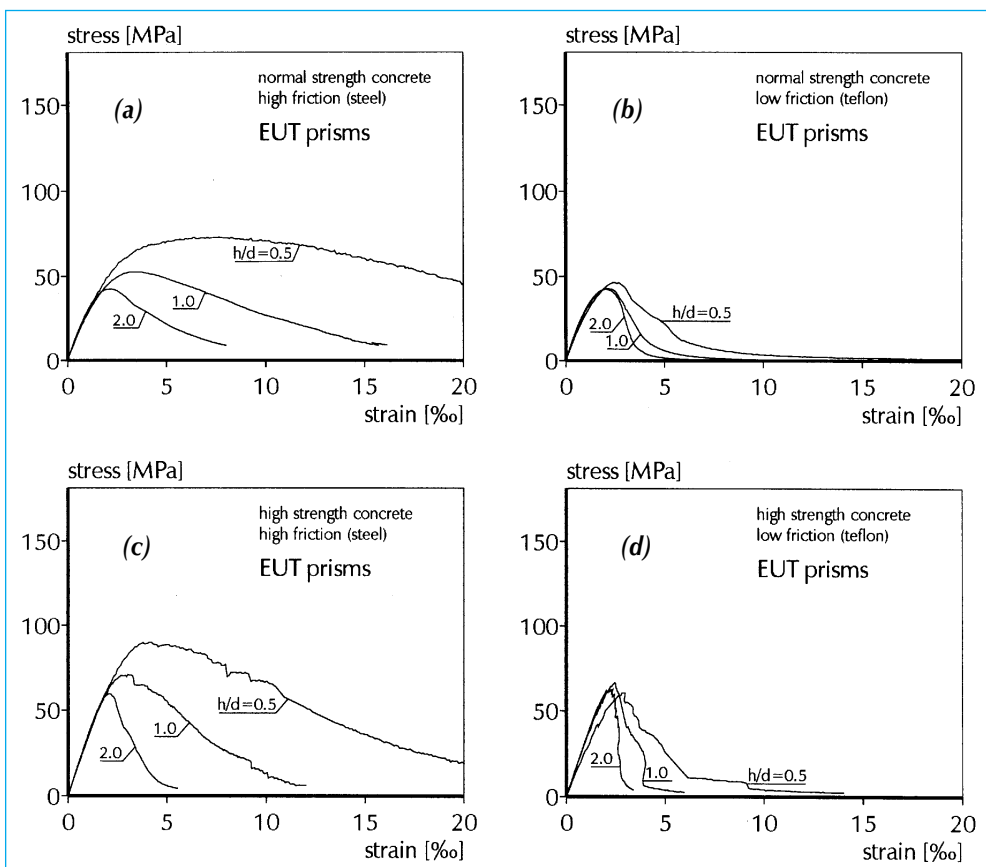


Fig. 9 – Stress-strain curves from prism tests carried out at EUT. Fig. (a) shows the results for normal strength concrete loaded between steel platens, (b) normal strength concrete between teflon platens, (c) high strength concrete between steel platens, and (d) high strength concrete between teflon platens, after Van Geel (1994).

when anti-friction measures were taken. At other laboratories difficulties were also encountered. As was mentioned before, due to the enormous energy release for high strength concrete, snap-back behaviour may be observed for some stress-strain diagrams. It all depends on the choice of control variable in the tests. We will return to these matters in Section 6.

An additional result from SINTEF, concerning a high strength concrete of 109.3 MPa, is shown in Fig. 11. Although these results were slightly beyond the scope of the Round-Robin (cylinders with $h/d = 2, 3$ and 4 were tested, and only rigid steel platens were used), they are of interest as they show the increase of ductility with decreasing slenderness for this material too, although the effect seems to be less as for the lower strength concretes. The SINTEF tests were controlled by a combined signal of axial and lateral deformations (Markeset (1995)), which allowed detecting stable softening behaviour. Note that for $h/d = 2, 3$ and 4 , the decrease of strength is not very significant for tests between rigid steel platens. This can also be observed from Fig. 5, where a plateau is reached when $h/d > 2$.

When the stress-strain curves of Figs. 8 through 11 are compared, it can be seen that the DUT results seem to have a higher initial stiffness. This is only an optical effect due to the longer x-axis. Most test series were quite consistent as far as the overall shape of the stress-strain curve was concerned. Exceptions were found in the test series carried out at THD and UM. Part of the reason seems to be the use of two fixed loading platens in the test machines, at least for

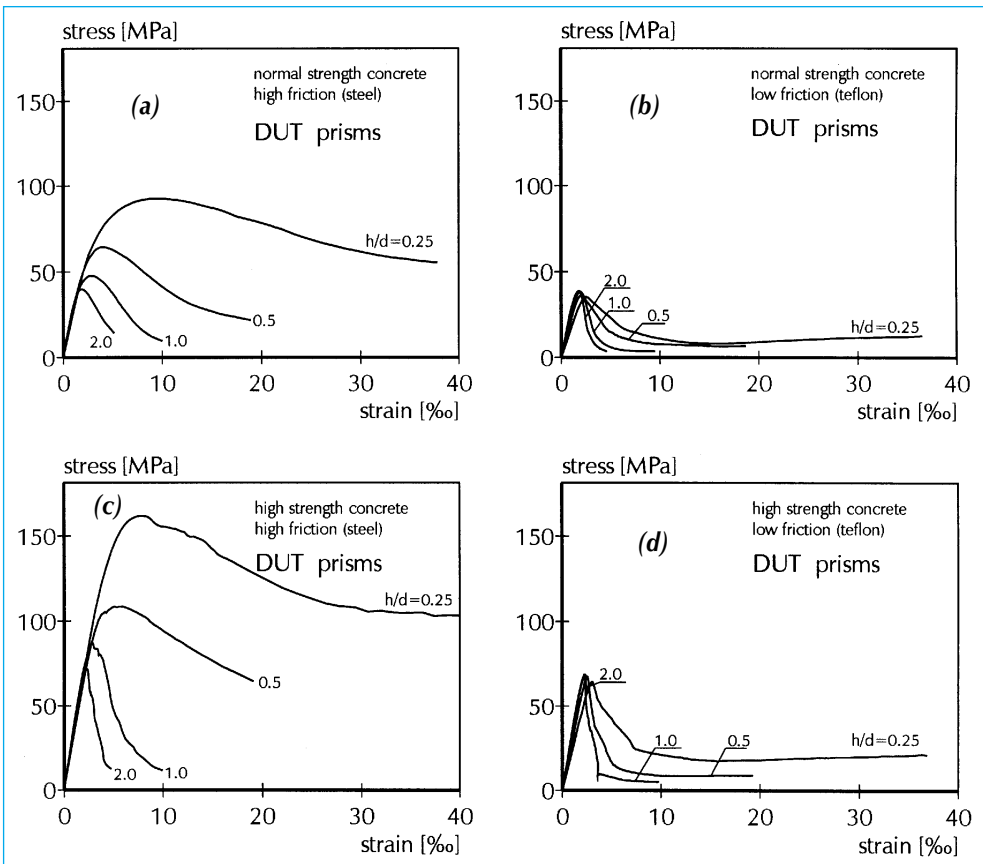


Fig. 10 – Stress-strain curves from prism tests at DUT. Fig. (a) shows the results for normal strength concrete loaded between steel platens, (b) normal strength concrete between teflon platens, (c) high strength concrete between steel platens, and (d) high strength concrete between teflon platens, after Van Vliet and Van Mier (1995). Note that in these tests the length of the x-axis is twice as long as used in all other figures. This was because of the extreme ductile behaviour of the 25 mm high specimens, which were added to the Round Robin test in the Stevin Laboratory.

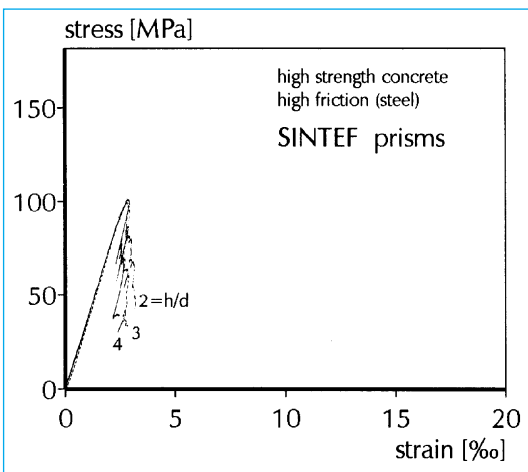


Fig. 11 – Stress-strain curves for high strength concrete, after Markeset (1995).

UM. Eccentricities, for example caused by non-orthogonal specimens, may have a significant effect on the results in such test set-ups. Normally this results in a rather large scatter of test results. Again at Darmstadt and Minnesota, the variability between test results was largest. This suggests that a hinge is certainly no luxury in a compression machine, and that a careful specimen manufacturing method is very important as well. However, when the loading apparatus is fitted with two fixed loading platens, one might decide to use a capping between specimen and

loading platens to overcome this problem.

5.2.2 Effect of boundary restraint

The effect of boundary restraint will be most significant in specimens having a small slenderness ratio h/d , see Fig. 7. The unrestrained zones should almost diminish when frictionless loading platens are used, but the question remains if the concrete is then tested under the identical circumstances in which it is used, for example, in a reinforced concrete structure. The best loading situation does not perhaps exist, as in the ideal situation the frictional restraint between loading platen and specimen should always be minimized, *i.e.* during the entire fracture process from individual microcrack nucleation and growth to full scale macrocracking. This is quite a severe condition. Lubricated platens like teflon exhibit a so-called stick slip behaviour, and before almost unrestrained sliding may occur, quite some restraint has to be overcome. In practice, the build-up of restraint will occur in the pre-peak regime of the stress-strain curve and may have some effect on the peak stress.

Beyond peak, sliding is almost unrestrained, and a frictional coefficient of 0.01 may be obtained. In Fig. 12, an example is given of the frictional restraint caused by the teflon platen used at EUT.

Other loading systems act differently. For example, brush bearing platens reduce frictional restraint by bending of the individual brush rods when lateral deformations of a specimen occur. When the lateral deforma-

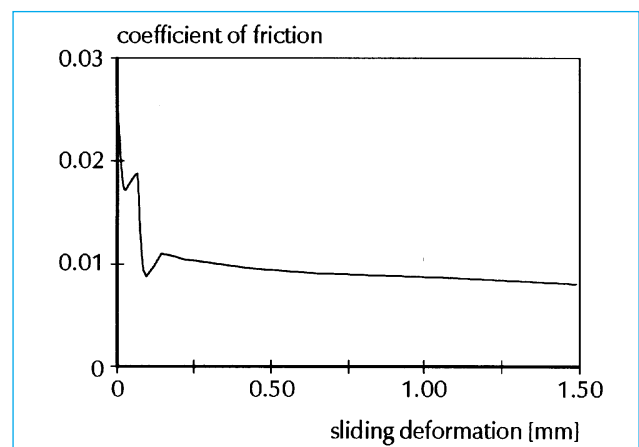


Fig. 12 – Frictional restraint of a teflon platen used at EUT, after Vonk (1992).

tions increase in magnitude, the brush rods want to return to their original straight position and frictional restraint will develop. Thus, in contrast to the teflon platen, a gradual build-up of frictional restraint develops, which must be most prominent in the post-peak regime of the stress-strain curve. This means that brushes must be considered preferable to teflon in the pre-peak regime, but in the post-peak regime, the teflon platen seems a better choice.

It is obvious that a change of loading platen during a test is virtually impossible. Therefore, to develop constitutive laws for concrete, it seems appropriate to apply a method of inverse modelling to subtract the “real” properties of the material, rather than to try to measure the softening properties of concrete directly. In such an inverse approach, it seems best to compare the response of concrete specimens loaded between different loading systems with widely-varying boundary restraint. In the present Round-Robin, such a large variation is present because the selection of a frictionless boundary was left to the competence of the individual contributors. Table 3 gives an overview of all the different systems used. The scope of the tests carried out at INSA and NTUA/IC deviated from the Round Robin proposal, but provide an excellent view of the diversity of specimen behaviour which can be measured with different loading systems. Most of the other laboratories used teflon layers, a combination of teflon and grease, or only grease as a friction-reducing medium (Note: a warning about the effect of applying excessive grease between the steel loading platen and the concrete specimen was given in Fig. 1). The thickness of the teflon layers varied from 50 μm to 1000 μm . At US, the effect of varying the thickness of the teflon layer was studied and the results will be shown below.

Let us first consider the effect of load application on the stress-strain behaviour in compression. INSA carried out tests between four different platens, namely plain steel, teflon, brass and aluminium. The last two systems were combined with talc powder. In Fig. 13 a, comparison is made between the stress-strain curves obtained with these four systems for normal strength concrete. The specimens were 118 mm cylinders. The brass and aluminium loading platens give a reduction of ductility as compared to the rigid steel platens. However, this

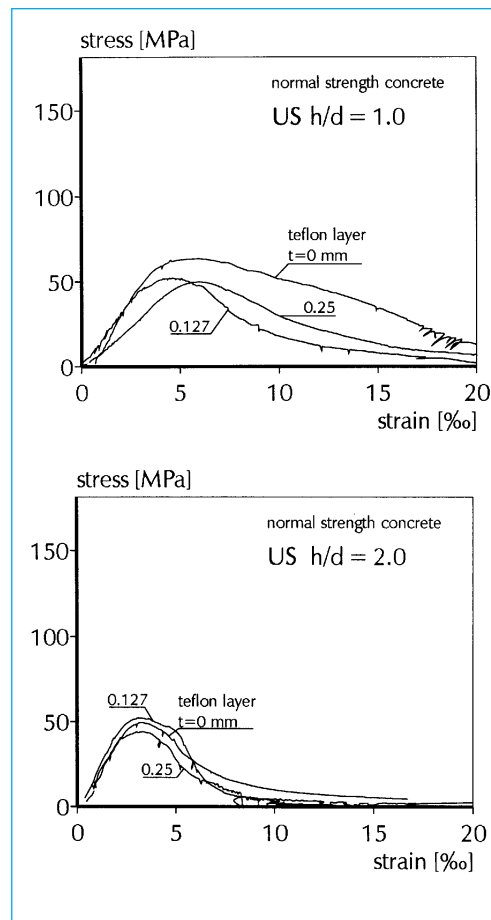


Fig. 14 – Effect of teflon thickness from test data of US, after Lange-Kornbak and Karihaloo (1994).

reduction is only marginal. In this respect, the effect of the teflon is much more pronounced, and an enormous decrease of strength is measured together with a significant reduction of ductility. The difference is as marked as was shown before in Figs. 8 through 10. The teflon platen at INSA was comprised of two 1 mm thick sheets.

The effect of the thickness of the teflon layer on the stress-strain behaviour of prismatic specimens with $h/d = 1.0$ and 2.0 was studied at US. There, however, only a single sheet of teflon was applied, and the thickness varied between $t = 0, 0.127$ and 0.254 mm. The results are shown in Fig. 14. The largest difference is found between $t = 0$ mm (plain steel platen) and $t = 0.127$ mm. A further increase of the teflon thickness has only a marginal effect. This seems to indicate that it does not really matter what kind of teflon platen is used, at least as long as no grease is applied.

At THD, ACBM, EUT and DUT, grease was applied either between the teflon and the steel (EUT) or between two teflon sheets (DUT, THD). At DUT, the grease was applied using a simple device through which the amount of grease applied could be held constant, see Van Mier (1997). It is recommended that such a device be included for a future test recommendation on strain softening under uniaxial compression. At THD, EUT and also in the tests at ACBM and UM, the application of grease was possibly not very well controlled. This may, in the case of UM and THD, have added to the increase of the scatter (in addition the effect of geometric imperfections in combination with a loading machine having two fixed loading platens). These last remarks are rather speculative and are meant to warn

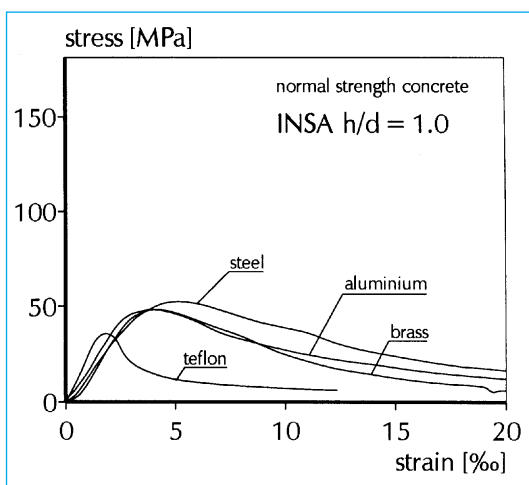


Fig. 13 – Effect of loading platen on the stress-strain behaviour in uniaxial compression, test data from Bascoul *et al.* (1994).

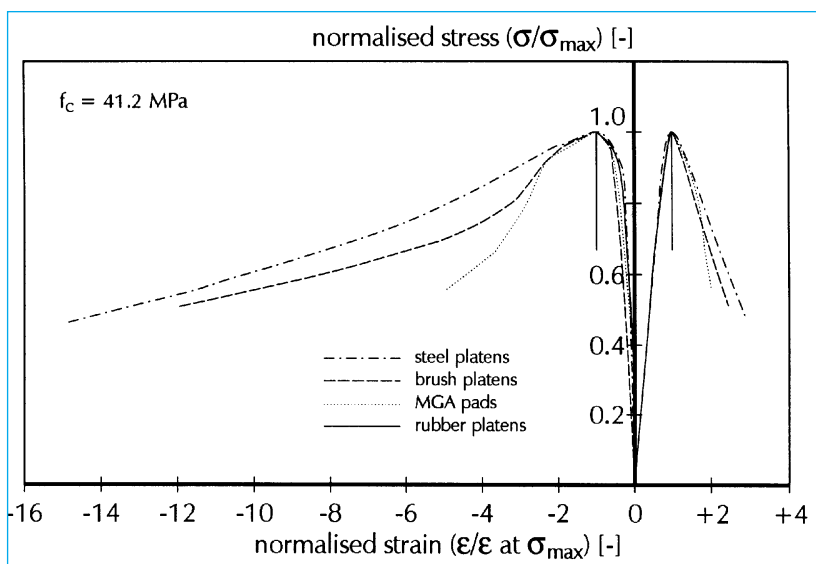


Fig. 15 – Effect of loading platens on the normalised stress-strain diagram of concrete in compression, after Zissopoulos *et al.* (1994).

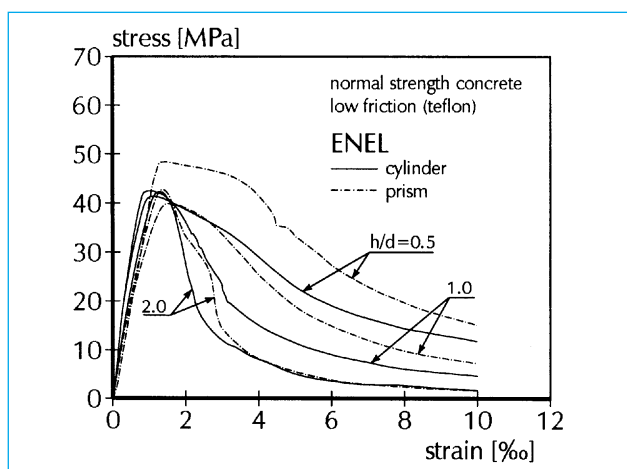


Fig. 16 – Comparison of stress-strain curves from cylinder tests and prism tests between teflon platens. Data from Gobbi and Ferrara (1995).

about such effects. In a future recommendation, the description of the compression test for strain-softening should be written in such a way as to avoid these undesired effects.

Finally, in Fig. 15 results obtained at NTUA/IC are shown. The tests did not conform to the Round Robin proposal, but the effect of loading platens on stress-strain behaviour is quite clear and confirms the above. At NTUA/IC, rubber, MGA pads (a sandwich layer, see Table 3) and brushes were compared to tests between rigid steel platens. The rubber platen can be quite hazardous, as the frictional restraint may be reversed, similar to what was indicated in Fig. 1. It all depends on the quality of the rubber inserted. For the purpose of inverse modelling, such “extreme” tests are quite helpful, provided of course that the frictional characteristics of the rubber platen are determined and supplied to the analysts. Note that the rubber test shows an almost vertical softening branch in Fig. 15. This may indicate either a reversal of frictional restraint or that the system is most effective. A definite conclusion is hard to reach as long as no further details about the fric-

tional characteristics of the rubber platen are known. Fig. 15 is the only figure that shows the lateral deformations. They increase at a faster rate beyond peak when the effectiveness of the frictionless loading platen is increased (*i.e.* when boundary restraint is reduced).

The tests carried out at DUT indicated that scatter decreases when teflon platens are used instead of rigid steel platens, see Van Vliet and Van Mier (1996). This may plead for a recommendation using a simple teflon platen in uniaxial compression tests for the determination of the stress-strain curve including the softening behaviour. RILEM Committee 148-SSC will propose a draft recommendation to be published in *Materials and Structures* in the near future.

5.3 Geometrical effects on stress-strain behaviour

Originally the geometry of the test specimen was not to be considered in the Round Robin. Fortunately, however, the shape (cylinders versus prisms) and size of the specimens were considered at THD and ENEL. In Section 5.3.1, we will discuss the effect of specimen shape on the stress-strain behaviour, whereas in Section 5.3.2, ENEL's results from prisms with different sizes are shown.

5.3.1 Prisms versus cylinders

The results of the various test series from the different laboratories differed markedly. Therefore, a comparison only between prismatic specimens and cylindrical specimens seems to make sense if the specimens are tested under the same conditions in a single laboratory. The effect of specimen shape will be shown only by giving some of the ENEL test results. The absolute values, and to some extent the shape of the stress-strain curves, may change when the same geometrical variation is tested in another laboratory. Based on the above global comparison, one may expect that the tendencies remain the same. In Fig. 16 a comparison is made between the prism and cylinder tests carried out at ENEL. The specimen diameter was 100 mm. Teflon was used as a friction-reducing layer. The results indicate that the variation in peak strength is larger for the prism tests. The cylinders appear to give lower strengths than the prisms, which would not be expected when stress-concentrations along edges and at corners of prismatic specimens are concerned. The reason for this is not clear and one may only speculate. A numerical analysis might be helpful to elucidate the deviations. The variation of post-peak ductility with slenderness, however, does not seem affected by using either prismatic or cylindrical specimens.

5.3.2 Specimen size

At ENEL the variation of prism size was also studied. Prisms of three slenderness ratios $h/d = 0.5, 1.0$ and 2.0 , but also having varying cross-section, $d = 50, 100$ and 150 mm, were tested. The results have been gathered in Fig. 17. Basically, the curves all seem to indicate the same behav-

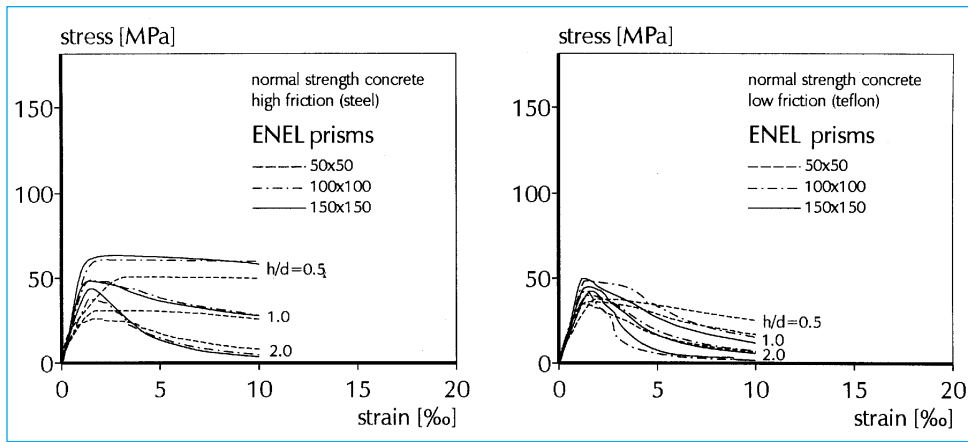


Fig. 17 – Comparison of stress–strain curves for prisms of different sizes, different slenderness ratios h/d and loaded between rigid steel platens (left diagram) or teflon platens (right diagram). Test-data from Gobbi and Ferrara (1995).

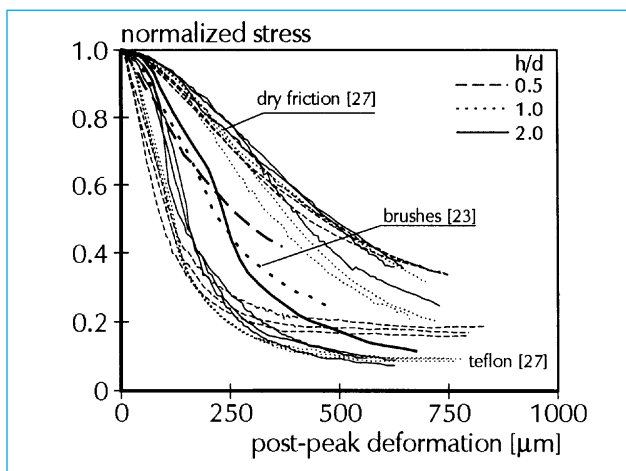


Fig. 18 – Stress–post peak deformation diagrams for uniaxial compression tests on prisms with varying slenderness h/d and loaded between different types of loading platens, after Van Vliet and Van Mier (1996).

our. As described by Gobbi and Ferrara, the smaller specimens were more difficult to centre in the compression machine. Apart from that, the aforementioned post-peak behaviour is confirmed for all three specimen sizes.

5.4 Post-peak localization

All stress–strain diagrams where tests with different slenderness are compared, *i.e.* Figs. 8–10 and 16–17, indicate an increase of ductility with decreasing slenderness. Earlier tests (Van Mier (1984, 1986)) revealed that post-peak localization of deformation occurs in uniaxial compression, which means that the same post-peak displacement is measured irrespective of the specimen height. The test results from the Round Robin indicate the same tendency. In Fig. 18, stress–post peak deformation diagrams are shown for tests between teflon, brushes and plain steel platens (dry friction). The results for specimens of different slenderness are plotted, *i.e.* $h/d = 0.5, 1.0$ and 2.0 . Quite clearly, results of tests with different slenderness, but loaded with the same type of loading system, are located in a relatively narrow bundle. Thus, on the basis of this diagram it can be

concluded that post-peak localization of deformations occurs irrespective of the type of loading system. This trend is confirmed by the tests of all participants, as is made clear by all the foregoing figures.

6. ABOUT FEED-BACK SIGNALS

As mentioned before, for compressive testing of high strength concrete, special measures must be

taken to register the complete softening diagram. Different strategies can be used to ensure stable softening, such as closed-loop testing using another control parameter than the usual deformation in the direction of the applied load. Stable softening diagrams were, among others, measured at ACBM. A test result is included in Fig. 19. Fully normalized stress–strain curves for high strength concrete tests on specimens of varying slenderness are shown. The tests were controlled using the circumferential strain, which was measured using a circumferential gauge consisting of a chain and an extensometer, as the feed-back signal. If such control had not been used, failure of all specimens would have occurred at the first snap-back point, *i.e.* where both the stress and strain decrease (provided, of course, that conventional deformation–control over the

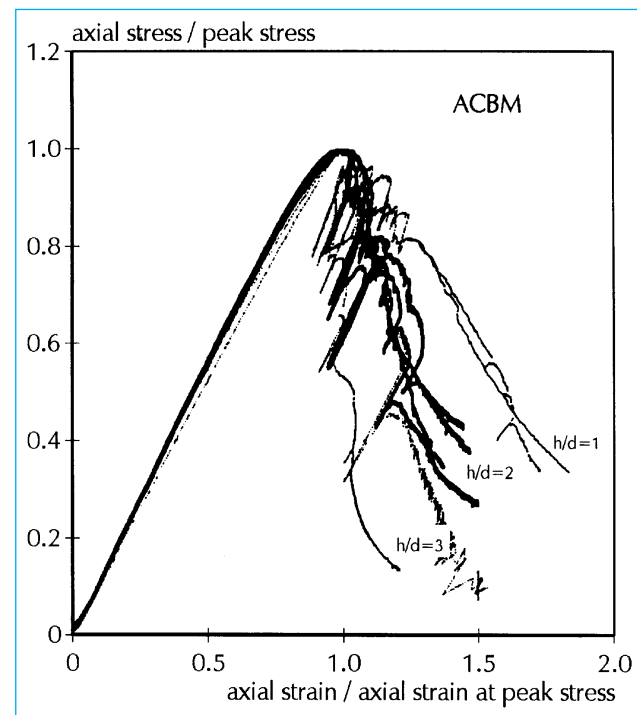


Fig. 19 – Normalized stress–strain curves for high strength concrete tests loaded between plain steel platens, after Choi *et al.* (1994). Circumferential strain–control was used for measuring stable post-peak response.

axial deformation was used). The high strength concrete tests at, for example, THD and DUT suffered from instabilities as soon as $h/d > 2.0$ and load was applied through teflon platens (see, for example, the $h/d = 2.0$ test in Fig. 8d). Note that at THD tests with alternative feed-back signals allowed measuring stable strain-softening curves of high strength concrete as well. In the THD tests, but also at SINTEF (Fig. 11), the tests were controlled through a signal which was a combination of axial and lateral deformation. At EUT, a combination of axial load and axial deformation was successfully used for measuring strain softening of high strength concrete. All such measures should be included in the draft recommendation for the determination of strain-softening of concrete under uniaxial compression. However, it should be mentioned that the procedures are not very straightforward, and experience in such tests must be developed through trial and error.

7. CONCLUSIONS

In this report, an overview is given of the results obtained from an extensive Round Robin test programme on strain-softening of concrete under uniaxial compression. Tests were conducted at ten different laboratories from around the world, which provided an extensive data base for establishing a standard test method for a new draft recommendation to measure softening of concrete under compression. The strength of concrete, in either normal strength concrete or high strength concrete, is dependent on the type of loading platen used and the slenderness of the specimen. With decreasing slenderness, an increase of specimen strength is measured when rigid steel loading platens are used. In contrast, when friction-reducing measures are taken, for example by inserting a sheet of teflon between the steel loading platen and the concrete specimen, the specimen strength as measured from prisms or cylinders becomes independent of the slenderness ratio h/d . The pre-peak stress-strain behaviour was independent of the slenderness when low-friction loading platens were used. In the softening regime, however, an increase of ductility (in terms of stress and strain) with decreasing specimen slenderness was found in all experiments. Close

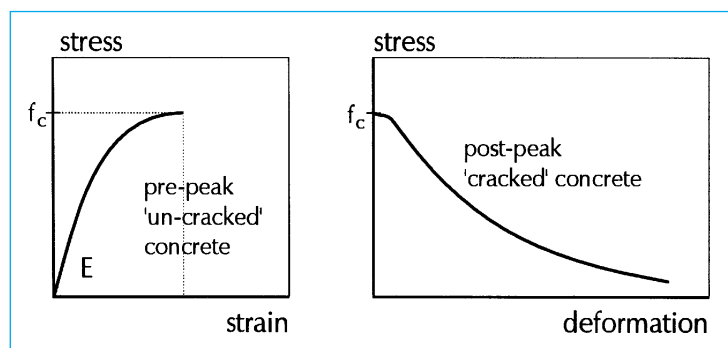


Fig. 20 – Pre-peak behaviour of ‘un-cracked’ concrete and post-peak softening behaviour of ‘cracked’ concrete. Cracked concrete contains cracks that are visible to the naked eye, whereas ‘un-cracked’ concrete may contain micro-cracks that cannot be observed by the naked eye.

observation of the stress-post peak deformation curves showed that a strong localization of deformations occurs in the softening regime, irrespective of the loading system used. The Round Robin test programme confirms the earlier results by Van Mier (1984).

For structural applications, it seems important to consider the pre- and post-peak parts of the stress-deformation diagram independently, as clarified in Fig. 20. The ascending branch of the stress-strain curve describes the behaviour of *un-cracked* concrete (*i.e.* cracks not visible to the naked eye), whereas the softening branch is associated with the behaviour of *cracked* concrete (*i.e.* cracks visible to the naked eye). The behaviour of macroscopically-cracked concrete is affected by the structural environment, as was clearly shown in the Round Robin test programme.

The Round Robin results indicate that reliable and reproducible strain-softening behaviour of concrete under uniaxial compression can be measured for specimens of relatively high slenderness ($h/d = 1.0-2.0$), loaded between teflon platens. A recommendation for such a test shall be given in a forthcoming RILEM recommendation. This recommendation should, in addition to a full description of the experiment and the test specimen, include a proposal for measuring strain-softening of high strength concrete. Clearly, for high strength concrete additional measures must be taken, as was shown convincingly by a number of participants in the Round Robin.

ACKNOWLEDGEMENTS

The authors would like to acknowledge the contribution of Dr. D.C. Jansen in supplying information for Section 4.4. The valuable comments of the contributors and committee members are very much appreciated and were used to improve the manuscript.

REFERENCES

- [1] Bascoul, A., Arnaud, M., Balayssac, J.P. and Turatsinze, A., ‘Strain Softening Behaviour of Concrete - Round Robin Test’ (INSA Toulouse, December 1994) 20 pp.
- [2] Choi, S., ‘Fracture Mechanism in Cement-Based Materials under Compressive Loads’, PhD Thesis, Northwestern University, Evanston, IL, USA, 1996.
- [3] Choi, S., Thienel, K.-C. and Shah, S.P., ‘Strain Softening of Concrete - RILEM Round Robin Test’ (NSF-ACBM, Northwestern University, Evanston, IL, USA, July 1994) 50 pp.
- [4] Dahl, H. and Brincker, R., ‘Fracture energy of high strength concrete in compression’, in ‘Fracture of Concrete and Rock - Recent Developments’, Barr, B. *et al.* Eds. (Elsevier Applied Science, London/New York, 1989) 523-536.
- [5] Dasenbrock, D., Labuz, J. and French, C., ‘Strain Softening of Concrete in Uniaxial Compression’, (Department of Civil Engineering, University of Minnesota, Minneapolis, MN, USA, July 1995) 23 pp.
- [6] Gerstle, K.H., Linse, D.L., Bertacchi, P., Kotsovos, M.D., Ko, H.-Y., Newman, J.B., Rossi, P., Schickert, G., Taylor, M.A., Traina, L.A., Zimmerman, R.M. and Bellotti, R., ‘Strength of concrete under multiaxial

- stress states', in Proceedings Douglas McHenry Int'l. Symposium on 'Concrete and Concrete Structures', ACI SP 55, American Concrete Institute, Detroit, 1978, 103-131.
- [7] Glavind, M. and Stang, H., 'Evaluation of the complete compressive stress-strain curve for high strength concrete', in 'Fracture Processes in Concrete, Rock and Ceramics', Van Mier, J.G.M., Rots, J.G. and Bakker, A., Eds. (Chapman and Hall/E & FN Spon, London/New York, 1991) 749-759.
- [8] Gobbi, M.E. and Ferrara, G., 'Strain Softening of Concrete under Compression' (ENEL-CRIS, Milano, May 1995) appr. 250 pp.
- [9] Han, N. and Walraven, J.C., 'Sustained loading effects in high strength concrete', in 'Utilization of High Strength Concrete', Lillehammer, Norway, June 20-23, 1993, 1076-1083.
- [10] Hudson, J.A., Brown, E.T. and Fairhurst, C., 'Shape of the complete stress-strain curve for rock', in 'Stability of Rock Slopes', Cording, E.J., Ed. (ASCE, New York, 1972) 773-795.
- [11] Jansen, D.C., Shah, S.P. and Rossow, E.C., 'Stress-strain results of concrete from circumferential strain feedback controlled testing', *ACI Materials Journal* **92** (4) (1995) 419-428.
- [12] Jansen, D.C. and Shah, S.P., 'Effect of length on compressive strain softening of concrete' (1997) to appear in *ASCE J. Engng. Mech.*
- [13] König, G., Simsch, G. and Ulmer, M., 'Strain Softening of Concrete' (Technical University of Darmstadt, October 1994) 67 pp.
- [14] Kotsovos, M.D., 'Effect of testing techniques on the post-ultimate behaviour of concrete in compression', *Mater. Struct.* **16** (1983) 3-12.
- [15] Lange-Kornbak, D. and Karihaloo, B.L., 'Strain Softening of Concrete under Compression' (School of Civil and Mining Engineering, University of Sydney, Australia, November 1994) 60 pp.
- [16] Markeset, G., 'High Strength Concrete Phase 3E - SP4 - Comments on Size Dependence and Brittleness of HSC' (SINTEF Structures and Concrete, Trondheim, Norway, February 1995) 23 pp.
- [17] Okubo, S. and Nishimatsu, Y., 'Uniaxial compression testing using a linear combination of stress and strain as the control variable', *Int'l. J. Rock Mech., Min. Sci. and Geomech. Abstr.* **22** (5) (1985) 323-330.
- [18] Rokugo, K., Ohno, S. and Koyanagi, W., 'Automatic measuring system of load-displacement curves including post-failure region of concrete specimens', in 'Fracture Toughness and Fracture Energy of Concrete', Wittmann, F.H., Ed. (Elsevier Science Publishers, Amsterdam, 1986) 403-412.
- [19] Schickert, G., 'Schwellenwerte beim Betondruckversuch (Threshold Values in Compressive Tests on Concrete)', Deutscher Ausschuss für Stahlbeton, 312, (1980) Berlin (in German).
- [20] Shah, S.P., Gokoz, U. and Ansari, F., 'An experimental technique for obtaining complete stress-strain curves for high strength concrete', *Cement, Concrete and Aggregates (CCAGDP)* **3** (1) (1981) 21-27.
- [21] Taerwe, L.R., 'Influence of steel fibres on strain softening of high strength concrete' *ACI Materials Journal* **89** (1) (1992) 54-60.
- [22] Van Geel, H.J.G.M., 'Uniaxial Strain Softening of Concrete - Influence of Specimen Size and Boundary Shear' (Eindhoven University of Technology, Report BKO94.09, July 1994) 34 pp. plus appendices.
- [23] Van Mier, J.G.M., 'Strain Softening of Concrete under Multiaxial Compression', Ph.D Thesis, Eindhoven University of Technology, The Netherlands, November 1984.
- [24] Van Mier, J.G.M., 'Multiaxial strain-softening of concrete, Part I: Fracture, Part II: Load-Histories', *Mater. Struct.* **19** (1986) 179-191.
- [25] Van Mier, J.G.M., 'Proposal for a Round Robin Test, RILEM TC 148-SSC Strain Softening of Concrete', March 24, 1993.
- [26] Van Mier, J.G.M., 'Fracture Processes of Concrete' (CRC Press, Boca Raton, FL, 1997).
- [27] Van Vliet, M.R.A. and Van Mier, J.G.M., 'Strain-Softening Behaviour of Concrete in Uniaxial Compression' (Delft University of Technology, Department of Civil Engineering, Report no. 25.5-95-9, May 1995) 87 pp.
- [28] Van Vliet, M.R.A. and Van Mier, J.G.M., 'Experimental investigation of concrete fracture under uniaxial compression', *Mechanics of Cohesive-Frictional Materials* **1** (1996) 115-127.
- [29] Vonk, R.A., 'Softening of Concrete Loaded in Compression', Ph.D. Thesis, Eindhoven University of Technology, The Netherlands, 1992.
- [30] Vonk, R.A., Rutten, H.S., Van Mier, J.G.M. and Fijneman, H.J., 'Influence of boundary conditions on softening of concrete loaded in compression', in 'Fracture of Concrete and Rock - Recent Developments', Shah, S.P., Swartz, S.E. and Barr, B., Eds. (Elsevier Applied Science, London/New York, 1989) 711-720.
- [31] Zissopoulos, D., Pavlovic, M.N. and M.D. Kotsosvos, 'Strain Softening of Concrete - RILEM Round Robin Test' (Imperial College, London, and National Technical University of Athens, Greece, August 1994) 15 pp.